

Increases in c-Src Expression Level and Activity Do Not Promote the Growth of Human Colorectal Carcinoma Cells *In Vitro* and *In Vivo*^{1*}

Arkadiusz Welman, Christopher Cawthorne, Lourdes Ponce-Perez, Jane Barraclough, Sarah Danson, Stephen Murray, Jeff Cummings, Terry D. Allen and Caroline Dive

Cancer Research UK, Paterson Institute for Cancer Research, University of Manchester, Wilmslow Road, Manchester M20 4BX, UK

Abstract

The levels and activity of c-Src in colorectal cancer cells increase steadily during the course of colorectal carcinogenesis and are most highly elevated in advanced metastatic disease. However, the effects of increases in c-Src activity on the proliferation of colorectal cancer cells during early and late stages of tumorigenesis remain elusive. To study the consequences of increases in c-Src levels and activity on the growth of colorectal cancer cells in later stages of colorectal carcinogenesis, we developed human colorectal cancer cell lines in which c-Src levels and activity could be inducibly increased by a tightly controlled expression of wild-type c-Src or of the constitutively active mutant of c-Src, c-SrcY527F. Src induction activated multiple signaling pathways (often associated with a proliferative response) but promoted neither cell proliferation *in vitro* nor tumor growth in a xenograft model *in vivo*. These results indicate that, in more advanced stages of colorectal carcinogenesis, increases in c-Src levels and activity are likely to have functions other than the direct promotion of tumor growth.

Neoplasia (2006) 8, 905–916

Keywords: c-Src, colon cancer, proliferation, cell death, Tet On.

Introduction

The nonreceptor tyrosine kinase c-Src is a ubiquitously expressed 60-kDa protein that can regulate many signaling pathways involved in the control of cell proliferation, survival, differentiation, adhesion, and motility [1,2]. c-Src-mediated cell signaling is not restricted to its ability to act as a kinase but also involves its function as a scaffold for protein–protein interactions. Both kinase-dependent and kinase-independent functions of c-Src are regulated by multiple mechanisms and contribute to a plethora of cellular processes in a variety of cell types (reviewed in Thomas and Brugge [3] and Erpel and Courtneidge [4]). Abnormal c-Src protein levels and/or catalytic activities have been found in a number of human tumors, including breast, lung, skin, pancreas, and colon tumors [5–7].

In more than 70% of colorectal cancers, the levels and activity of c-Src are upregulated 5 to 40 times compared to neighboring normal mucosa and increase steadily in the course of tumor development, reaching the highest level in metastatic malignancies [2,8–11]. A high activity of c-Src has been correlated with poor clinical prognosis [12].

The functions of c-Src that are important in the early stages of colorectal carcinogenesis remain largely unexplored, not the least because model systems with which to investigate these are rare and technically challenging. Increases in c-Src activity in more advanced tumors seem to play a role in the modulation of cell–cell and cell–extracellular matrix interactions, and mounting evidence points to important function(s) of c-Src in invasion and metastasis [13–17].

Although the mitogenic response to v-Src signaling has been established in fibroblasts [1,2,18–20], uncertainty remains with regard to the impact of increased c-Src activity on colorectal cancer cell growth. The few studies that used colon cancer cell lines stably transfected with constitutively expressed mutants of c-Src did not provide conclusive answers to growth-related questions due to adaptation issues during the selection of stable clones and difficulties regarding matched control clones [15,21]. Using an inducible gene expression approach, we have been able to assess more directly the effects of increases in c-Src levels and activity on the growth of two human colorectal cancer cell lines that display significantly different morphologic and molecular characteristics (HCT116 and SW480) [22]. Our data support the hypothesis that, in more advanced stages of colorectal carcinogenesis, increases in c-Src levels and activity do not directly promote tumor cell growth. This finding has important clinical implications in view of considerable activity in the development and clinical testing of c-Src inhibitors as anticancer drugs.

Address all correspondence to: Arkadiusz Welman, PhD, Clinical and Experimental Pharmacology Group, Paterson Institute for Cancer Research, University of Manchester, Wilmslow Road, Manchester M20 4BX, UK. E-mail: awelman@picr.man.ac.uk

¹This study was supported by a Cancer Research UK program grant (C147) to C. Dive.

*This article refers to supplementary material, which is designated by "W" (i.e., Figure W1) and is available online at www.bcdecker.com.

Received 22 June 2006; Revised 22 September 2006; Accepted 26 September 2006.

Copyright © 2006 Neoplasia Press, Inc. All rights reserved 1522-8002/06/\$25.00
DOI 10.1593/neo.06475

Materials and Methods

Plasmid Vectors

The construction and properties of pN1p β -actin-rtTA2S-M2-IRES-EGFP, pBILuc, and pBILuc-Src527F plasmids have been described previously [23]; the pBILuc-wtSrc plasmid is identical to pBILuc-Src527F but contains wild-type (wt) *c-Src* instead of mutant *c-SrcY527F*. The super module vectors pSMVLuc-Src527F, pSMVLuc-wtSrc, and pSMVLuc-only were generated by *Asel*-based fusion of the pN1p β -actin-rtTA2S-M2-IRES-EGFP plasmid with Dox-inducible modules derived from pBILuc-Src527F, pBILuc-wtSrc, and pBILuc, respectively (Figure 1A).

Cell Culture and Transfection

HCT116 and SW480 cells were grown in McCoy's 5A and DMEM media (Gibco/Invitrogen, Paisley, UK), respectively. The media were supplemented with 10% fetal calf serum, 100 U/ml penicillin, and 100 μ g/ml streptomycin.

Transfections were performed by mixing 20 μ g of plasmid DNA with $\sim 2 \times 10^7$ cells suspended in 400 μ l of Optimem with Glutamax (cat. no. 51985-026; Gibco/Invitrogen) in a 4-mm electroporation cuvette (cat. no. ECU104; Equibio, Ashford, UK) and by electroporation (simple pulse, 260 V, 1050 μ F) using an Easyject Plus electroporator (Equibio).

Selection of Stable Cell Lines, Luciferase Assay, and Microscopy

Stable cell populations were generated by the selection of cells transfected with indicated pSMV plasmids in media containing 800 μ g/ml G418 (cat. no. 11811-031; Gibco/Invitrogen) for 14 to 16 days, followed by 7 to 10 days of growth in the absence of G418 and flow cytometric sorting of enhanced green fluorescent protein (EGFP⁺) cells. Single-cell clones were picked using sterile cotton buds after low-density seeding in Petri dishes and were expanded to establish independent cell lines suitable for Dox-regulated expression of luciferase (Luc-only clones) or luciferase in combination with wt *c-Src* (Luc-wtSrc clones) or *c-SrcY527F* mutant (Luc-Src527F clones). Established single-cell clones were screened for functionality by luciferase assay and Western blot analysis using anti-Src antibody.

Luciferase assays were performed using the Luciferase Assay System (cat. no. E1500; Promega, Madison, WI) following the manufacturer's instruction.

Light and fluorescent microscopy studies were carried out as described previously [24].

Electron microscopy was performed as described previously, with minor modifications [25]. (See supplementary information for a more detailed description.)

Doxycycline (Dox) Treatments

Dox (cat. no. 8634-1) was obtained from Clontech (Palo Alto, CA) and stored at -20°C as a 2-mg/ml stock in H₂O.

Cells were plated at 1×10^6 cells/3 ml of medium per well in six-well plates (Corning, Corning, NY). After 20 to 24 hours, the medium was replaced with 3 ml of fresh medium with or without 2 μ g/ml Dox. Detached and adherent cells were counted with a hemocytometer 24 to 30 hours later. Alternatively, the cells were dissolved directly in $2\times$ sodium dodecyl sulfate (SDS) sample buffer or cell lysis buffer (cat. no. 9803; Cell Signalling, Danvers, MA), and lysates were analyzed by SDS polyacrylamide gel electrophoresis (PAGE) and Western blot analysis.

Four-day \pm Dox growth curves were determined after seeding cells at 4×10^5 /3 ml of medium per well in six-well plates. After 24 hours (day 1), the medium was replaced with 3 ml of fresh medium with or without 1 μ g/ml Dox, and the cells were counted with a hemocytometer daily for 3 days.

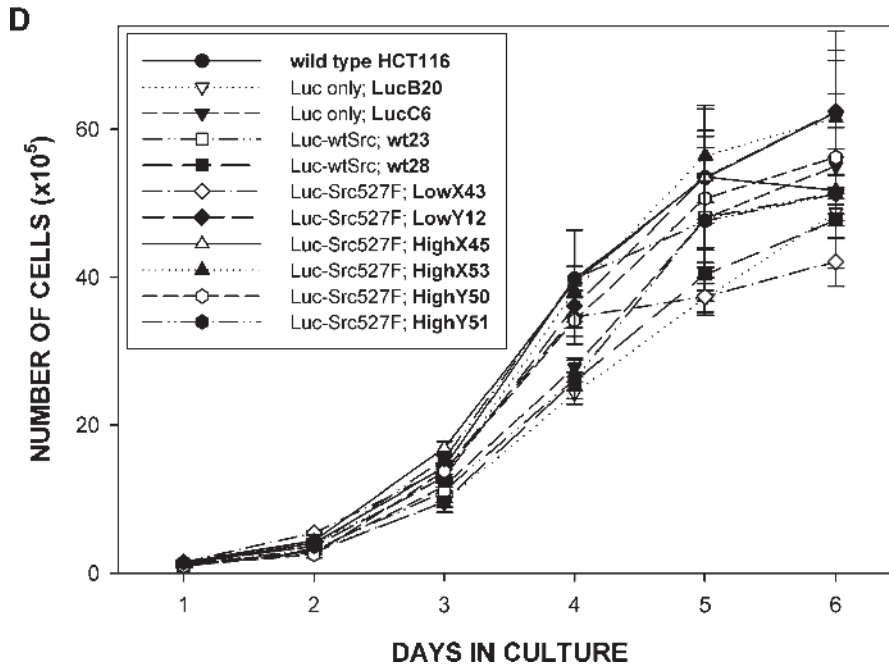
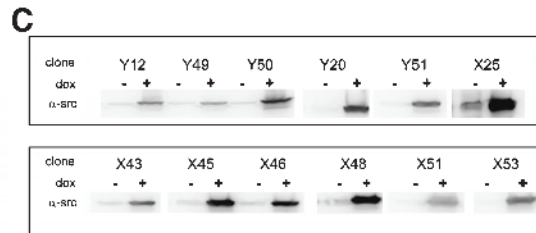
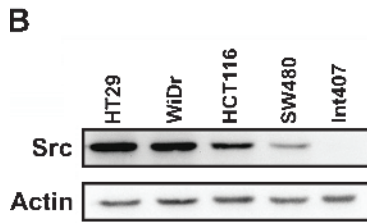
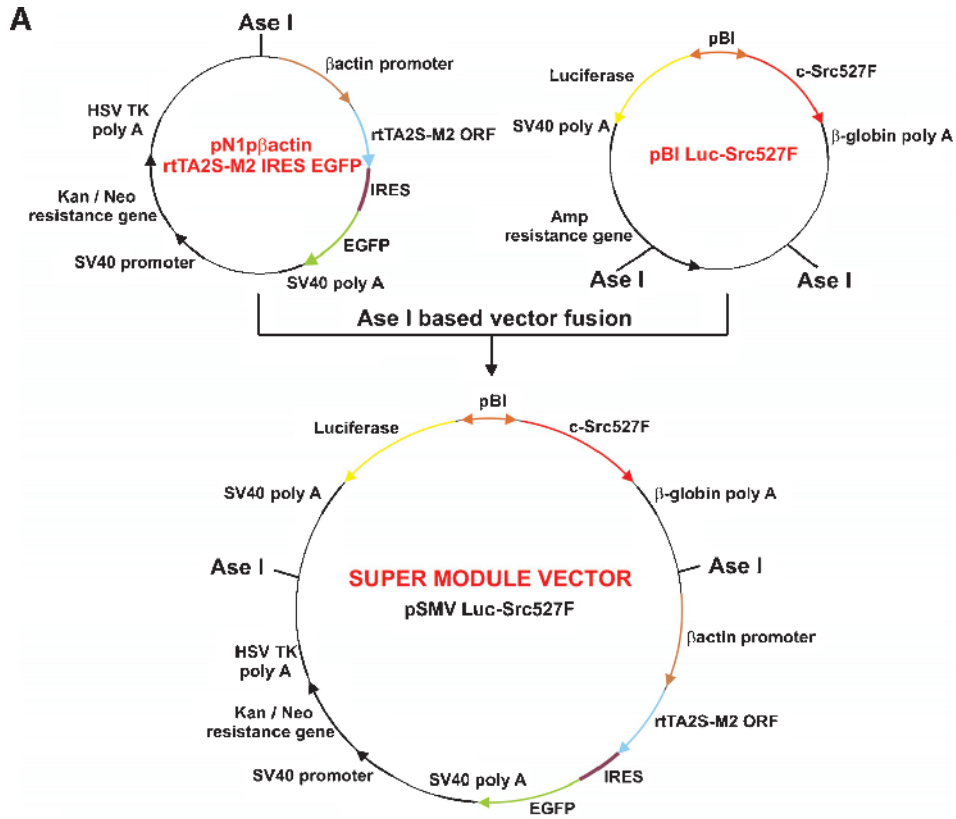
To establish whether HCT116 Luc-Src527F cells were able to overcome growth delay caused by high levels of *c-SrcY527F* mutant, HCT116 Luc-Src527F high clones (with Luc-only and parental HCT116 cells used as controls) at $\sim 70\%$ confluency in T75 tissue culture flasks were induced with Dox for 24 hours. Subsequently, the cells were split 1:1.5 to 1:4 every second day into new flasks containing fresh medium with Dox. Six to 8 days of such treatment resulted in a cell population that proliferated and displayed little cell detachment.

Detection of Apoptosis

Quantitation of cells displaying apoptotic nuclear fragmentation was performed by embedding adherent cells (grown on glass coverslips) and detached cells in Vectashield mounting medium containing DAPI (Vector Laboratories, Burlingame, CA) and by subsequently inspecting under a fluorescent microscope equipped with a DAPI filter.

M30-Apoptosense enzyme-linked immunosorbent assay (ELISA) assay is an ELISA for the quantitative measurement of apoptosis in cells of epithelial origin that express cytokeratin 18 (CK18; Peviva, Bromma, Sweden). Mouse monoclonal M30 antibody recognizes a neoepitope CK18-Asp396, which is exposed after the cleavage of CK18 by caspases [26]. The assay was performed as follows: cells were plated

Figure 1. Construction and use of super module vector for the induction of *c-SrcY527F* in human colon cancer cells. (A) Schematic illustrating the construction and structural features of the pSMVLuc-Src527F vector. The plasmid map of pSMVLuc-Src527F shows component elements of the vector, including a β -actin promoter-driven EGFP-linked module expressing rtTA2S-M2 transcriptional transactivator, a kanamycin/neomycin resistance cassette, and a bidirectional promoter-based module expressing luciferase and *c-SrcY527F* in a Dox-dependent manner. (B) Comparison of endogenous *c-Src* levels in HT29, WiDr, HCT116, and SW480 colon cancer cell lines. Int 407 cells represent a nontransformed human intestinal epithelial cell line [37]. (C) *c-SrcY527F* induction in representative HCT116 Luc-Src527F clones determined after 24 hours in the presence of Dox. (D) Growth characteristics of parental wt HCT116 cells and selected HCT116 Luc-only, Luc-wtSrc, and Luc-Src527F clones in the absence of Dox. Growth curves were determined after seeding 1×10^5 cells/well in six-well plates. Data are representative of three independent experiments performed in triplicate. Error bars represent standard deviations. For better transparency, the growth curves for each clone are also presented individually in Figure W4. Figure 1 contains a supplementary panel (Figure W1) illustrating the phosphorylation of diverse downstream effectors of *c-Src* in selected HCT116 clones in the presence and in the absence of Dox.



at 1×10^6 cells/well in six-well plates. After 24 hours, the medium was replaced with 2 ml of fresh medium containing 2 μ g/ml Dox, and cells were incubated for another 24 hours. Negative control consisted of cells in a medium without Dox, and positive control consisted of cells treated with staurosporine (35 nM) in the absence of Dox (this staurosporine concentration produced 50% apoptosis in HCT116 cells). Subsequently, 1 ml of medium was removed from each well and spun down at 1000 rpm for 5 minutes in a standard bench-top centrifuge, and the resultant supernatant was stored at -80°C before analysis. Each M30-Apoptosense assay kit contained a 96-well plate coated with a mouse monoclonal antibody to CK18, standards, quality controls, and reagents. Twenty-five microliters of each sample, control, or standard was pipetted into a well, and 75 μ l of horseradish peroxidase conjugate solution [mouse monoclonal M30 antibody in phosphate-buffered saline (PBS) with protein stabilizers] was added. The plate was then incubated for 4 hours at room temperature with constant shaking (600 rpm). Each well was washed five times with 0.1% PBS-T; 200 μ l of 3,3',5,5'-tetramethyl-benzidine substrate solution was added; and the plate was incubated in the dark for 20 minutes. The reaction was stopped by adding 50 μ l of 1 M sulfuric acid, and absorbance was measured in a microplate reader at 450 nm. The amount of M30 antigen in each sample was calculated by interpolation based on a five-point standard curve of known concentrations of M30 antigen.

Cell Cycle Analysis

Cell cycle analysis has been performed essentially as described previously, with minor modifications [23]. (See supplementary information for a more detailed description.)

Antibodies, Gel Electrophoresis, and Western Blot Analysis

SDS-PAGE was performed using 10% or 12.5% polyacrylamide gel. Proteins were blotted onto polyvinylidene fluoride membrane (PVDF) membranes (Perkin-Elmer, Boston, MA) and incubated with appropriate first antibody and horseradish peroxidase-coupled anti-mouse or anti-rabbit secondary IgG (Dako, Glostrup, Denmark). The following primary antibodies have been used: monoclonal mouse anti-v-Src (cat. no. OP07; Oncogene Research Products, Nottingham, UK); polyclonal rabbit anti-Src [pY⁴¹⁸] (cat. no. 44-660; Biosource, Camarillo, CA); polyclonal rabbit anti-Cdk1 (cat. no. 9112), polyclonal rabbit anti-P-Cdk1 (Tyr15) (cat. no. 9111), polyclonal rabbit anti-Erk1/2 (cat. no. 9102), monoclonal mice anti-P-Erk1/2 (Thr202/Tyr204) (cat. no. 9106), polyclonal rabbit anti-PKB (cat. no. 9272), polyclonal rabbit anti-P-PKB (Ser473) (cat. no. 9271), polyclonal rabbit anti-histone H3 (cat. no. 9715), polyclonal rabbit anti-P-histone H3 (Ser10) (cat. no. 9701), polyclonal rabbit anti-STAT3 (cat. no. 9132), and polyclonal rabbit anti-PSTAT3 (Tyr405) (cat. no. 9131; all from Cell Signalling); mouse monoclonal anti-paxillin (cat. no. 610051; BD Biosciences Pharmingen, San Diego, CA); rabbit polyclonal anti-paxillin [pY31] (cat. no. 44-720; Biosource); polyclonal rabbit anti-Src (cat. no. 44-6556; Biosource); and mouse monoclonal anti-actin (cat. no. A-4700; Sigma, Poole, UK).

Tumor Xenografts

HCT116 Luc-wtSrc 23 and HCT116 Luc-Src527F HighY50 cells were grown as subcutaneous xenografts in 8-week-old female Balb/c-NUDE nude mice (Paterson Institute for Cancer Research, Manchester, UK) following the injection of 5×10^6 cells in 0.1 ml of Optimem. Mice were housed in an individually ventilated caging system on a 12-hour light/dark environment maintained at constant temperature and humidity. The animals were fed a standard diet (controls) or a Dox-containing diet (625 mg/kg TD 01306; Harlan-Teklad, Madison, WI), and tumor volume (defined as length \times width \times height) was measured every second day. When tumor volume exceeded 800 mm³, the mice were sacrificed and samples of tumors were snap-frozen for subsequent luciferase assay. All procedures were carried out in accordance with UKCCR guidelines 1999 by approved protocol (Home Office Project license no. 40-2746).

Results

A Rapid, Single-Step, Nonviral System for Inducible Gene Expression in Cancer Cells

To investigate the consequences of increases in c-Src levels and activity on the growth of human colorectal cancer cells, we further enhanced the advantages of our recently reported two-step modification of the Tet On system [23,27]. By fusing the previously described pN1p β -actin-rtTA2S-M2-IRES-EGFP and pBILuc-wtSrc or pBILuc-Src527F plasmids, single super module vectors (pSMVLuc-wtSrc or pSMVLuc-Src527F, respectively) were obtained. They were designed for simultaneous Dox-dependent expression of the indicated c-Src protein (wt or constitutively active mutant) and firefly luciferase (used as reporter) (Figure 1A). These plasmids were transfected into HCT116 human colorectal cancer cells. HCT116 cells (similar to SW480 cells that will be described later) display relatively low levels of endogenous c-Src compared to some other colorectal cancer cell lines of similar stage and thus represent an appropriate model for functional studies on the effects of increases in c-Src levels and activity (see Figure 1B and the data presented in Dehm et al. [28]). Following selection in the presence of G418 and EGFP-based cell sorting (for details, see the Materials and Methods section), a large number (>100) of stably transfected clones were established. More than 25% of these clones displayed good Dox-driven inducibility with respect to wt c-Src or c-SrcY527F. The basal leakiness of gene expression in the majority of clones was very low or undetectable (Figure 1C and data not shown). For practical reasons, further studies were limited to two clones expressing wt c-Src (Luc-wtSrc clones wt23 and wt28), two clones expressing low levels of c-SrcY527F (Luc-Src527F clones LowX43 and LowY12), four clones expressing high levels of c-SrcY527F (Luc-Src527F clones HighX45, HighX53, HighY50, and HighY51), and two control clones established after the transfection of HCT116 cells with the pSMVLuc-only plasmid that expresses luciferase only (Luc-only clones LucB20 and LucC6). In the majority of experiments, we also included parental HCT116

cells as additional control. To our knowledge, the SMV system represents the first available single-step nonviral strategy ensuring a highly successful generation of tightly controlled Dox-inducible gene expression in a less tractable and more unpredictable human cancer cell context. As shown in Figure 1D, in the absence of induction, all selected cell lines displayed growth kinetics comparable to parental HCT116 cells, indicating that the genetic manipulations performed had not affected their basic growth characteristics.

Src Induction Activates Multiple Signaling Pathways

Src is known to influence multiple signaling pathways. As expected, inducible expression of wt c-Src and c-SrcY527F in HCT116 cells resulted in increased phosphorylation of several known downstream effectors, including other kinases (Erk and PKB/Act), the cytoskeletal protein paxillin, and the transcriptional regulator STAT3 (Figure W1).

Inducible Expression of wt c-Src and Low Levels of c-SrcY527F Do Not Effect the Proliferation of HCT116 Cells In Vitro

We examined the consequences of the expression of wt c-Src on cell growth. As shown in Figure 2, even induction of high levels of wt c-Src did not effect the proliferation of HCT116 cells, demonstrating that rises in c-Src levels per se are unable to confirm any proliferative advantage or disadvantage to these colorectal cancer cells. Considering the plentiful published studies performed using mouse or chicken fibroblasts that strongly indicated a need for sustained high Src activity to trigger reduction in cell doubling times and increased cell proliferation [1,2,18–20], we subsequently analyzed HCT116 clones expressing a constitutively active mutant of c-Src (c-SrcY527F). Initially, HCT116 Luc-Src527F LowX43 and LowY12 clones that are induced to express relatively low levels of c-SrcY527F (less than a 3-fold increase compared to endogenous c-Src for clone LowX43 and less than a 10-fold increase for clone LowY12) were examined (Figure 2A). Despite clear increases in the amount of active autophosphorylated c-Src following Dox-mediated induction, we did not observe any changes in cell proliferation kinetics or cell cycle profiles (Figure 2; Figure W2).

Inducible Expression of High Levels of c-SrcY527F Delays the Growth of HCT116 Cells In Vitro

Subsequently and again to reflect previous fibroblast-based studies with v-Src, we assessed the consequences of higher-level induction of c-SrcY527F on the growth of HCT116 cells. For these experiments, clones HCT116 Luc-Src527F HighX45, HighX53, HighY50, and HighY51, in which Dox-mediated induction of c-SrcY527F resulted in highly increased (>10 times) levels of total and autophosphorylated active c-Src (Figure 3B), were selected. Highly elevated levels of constitutively active c-Src resulted in spread of adherent cells, where a proportion of cells possessed large EGFP-free vesicular structures (Figure 3A). In addition, there was a clear increase in the number of cells that detached from monolayer (Figure 3, A and C). Control Luc-only and wt cells (similar to HCT116 Luc-wtSrc and Luc-Src527F Low

cells described in the Inducible Expression of wt c-Src and Low Levels of c-SrcY527F Do Not Effect the Proliferation of HCT116 Cells In Vitro section) did not display any changes in cell morphology when treated with Dox (Figure 3A), nor did they display any increased detachment (Figure 3C). When cells were counted 24 to 72 hours postinduction, the total number of cells in induced Luc-Src527F High clones was significantly lower than that in the same untreated cells (Figure 3, C and D). Over the same period of time, there were no differences between induced and uninduced samples within control Luc-only cell lines and parental HCT116 cells (Figure 3, C and D), suggesting that high increases in levels of constitutively activated c-Src had negative consequences on the growth of HCT116 cells *in vitro*. A more detailed analysis demonstrated that this resulted from accumulation in the G₂ phase of the cell cycle (confirmed by cell cycle profile, increased phosphorylation of Cdk1 on Tyr15, and decreased phosphorylation of histone H3 on Ser10) and occurrence of a nonapoptotic form of cell death (confirmed by M30-Apoptosense ELISA assay, DAPI staining, and electron microscopy) (Figure 4; Figure W3).

The identification of negative effects of high levels of c-SrcY527F on the *in vitro* growth of HCT116 cells was somewhat surprising considering that previous studies with v-Src in fibroblasts predicted the opposite effect and considering the fact that stable colorectal cancer cell lines that highly overexpress this constitutively active mutant of c-Src have been described in the past [15,29]. The ability of HCT116 cells to overcome c-SrcY527F-dependent growth delay when exposed to high levels of this activated c-Src mutant over prolonged periods of time was explored. The growth delay phenomenon appeared to last for 6 to 8 days when Dox-induced Luc-Src527F High clones were seeded at high density and split every second day. During this time, many cells died and were discarded. The fraction of cells that survived (mimicking perhaps the selection of stable clones) proliferated, and the rate of cell detachment decreased. The morphology of these cells (continuously induced and thus still overexpressing constitutively active Src) more closely resembled that of cells before c-SrcY527F induction (Figure 5A). To determine whether increased levels of constitutively active c-Src had any effect on the growth of these continuously induced cells, their growth properties were assessed in the presence and in the absence of Dox and were compared to those of control Luc-only cells and parental HCT116 cells under identical conditions. If at all, c-SrcY527F maintained reduced growth delay and certainly did not promote cell proliferation (Figure 5B). Thus, our studies to this point showed that induced expression of wt c-Src or of low levels of c-SrcY527F does not promote the proliferation of HCT116 cells and that high-level induction of this active mutant delays growth and promotes nonapoptotic cell death.

Inducible Expression of Activated Src Does Not Promote the Growth of SW480 Cells In Vitro

To confirm if lack of the growth-promoting effects of elevated Src activity observed in HCT116 cells was not a cell type-specific phenomenon, several Luc-Src527F clones

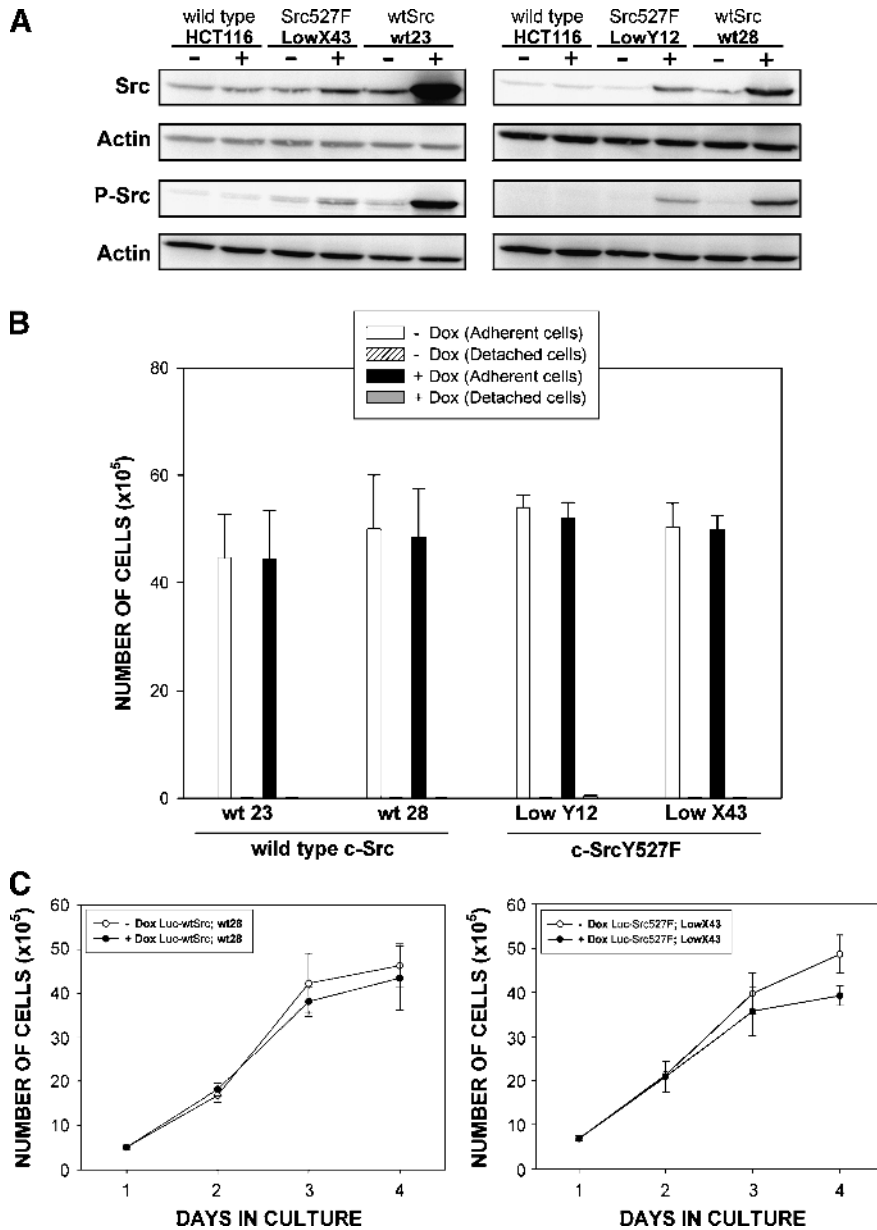


Figure 2. Consequences of the overexpression of wt c-Src and the low-level induction of c-SrcY527F in HCT116 colorectal cancer cells. (A) Western blot analyses illustrating the levels of total and autophosphorylated active Src [Tyr416] in indicated clones 24 hours after induction. (B) Histogram showing no changes in cell proliferation 24 hours following high-level induction of wt c-Src (clones wt23 and wt28) and low-level induction of c-SrcY527F (clones LowX43 and LowY12). Data are based on three independent experiments performed in triplicate. No statistically significant differences were found between numbers of cells in the presence and in the absence of Dox for any of the clones (two-sided t-tests, $P > .05$). (C) Four-day growth curves of HCT116 Luc-wtSrc (clone wt28) and HCT116 Luc-Src527F (clone LowX43) cells grown in the absence and in the presence of Dox. The initial seeding density was 4×10^5 cells/well. Data are representative of three independent experiments performed in triplicate. The cell cycle profiles of HCT116 Luc-wtSrc cells and HCT Luc-Src527F Low cells are presented in Figure W2.

were generated in the SW480 human colon cancer cell background. SW480 cells differ significantly from HCT116 cells with respect to molecular abnormalities associated with transformed phenotype. We were able to establish SW480 cells inducing low and high levels of activated c-Src. Similar to the results obtained in HCT116 cells, in SW480 cells, low-level induction of c-SrcY527F did not have any noticeable effects on cell proliferation, whereas high-level induction was growth-inhibitory (Figure 6).

Neither Induction of wt c-Src Nor Induction of c-SrcY527F Promotes the Growth of HCT116 Tumor Xenografts

The experiments described so far demonstrated that increases in the levels and activity of c-Src do not promote the proliferation of HCT116 and SW480 cells *in vitro*. To assess the consequences of Src upregulation on cell growth in a more complex *in vivo* microenvironment, we grew HCT116 clones inducing wt c-Src and constitutively active c-SrcY527F mutant (HCT116 SMVLuc-wtSrc wt23 and HCT116

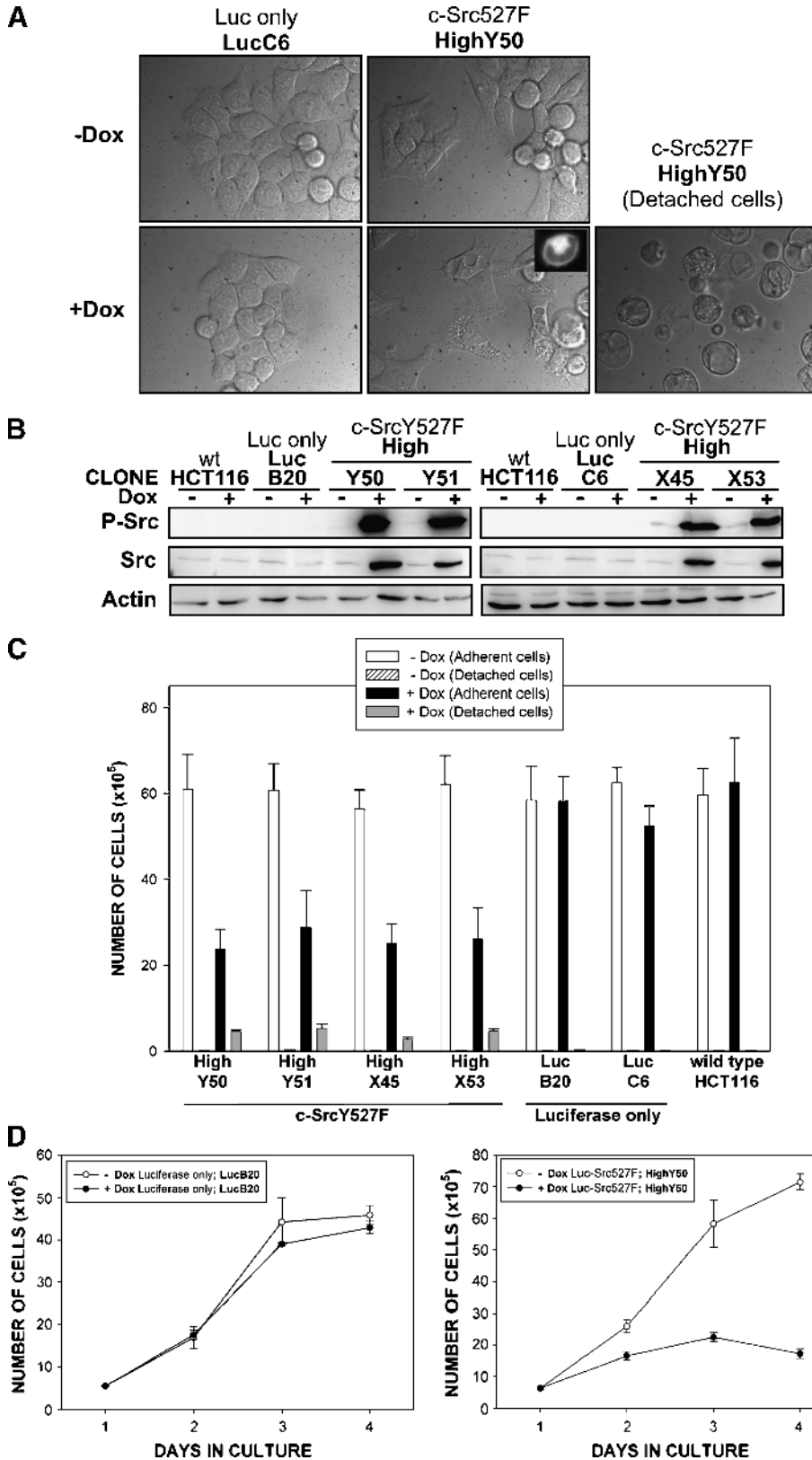


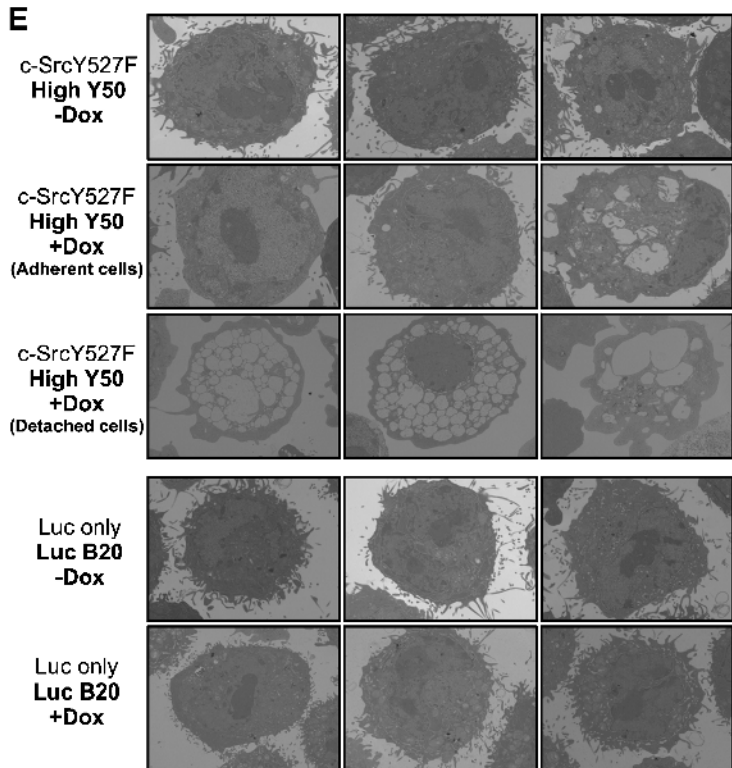
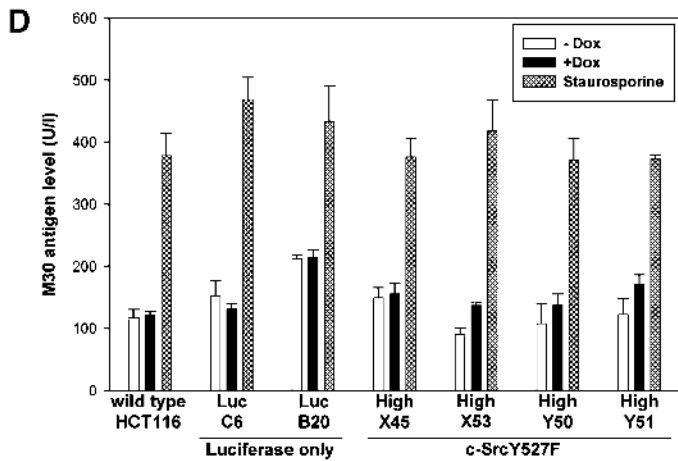
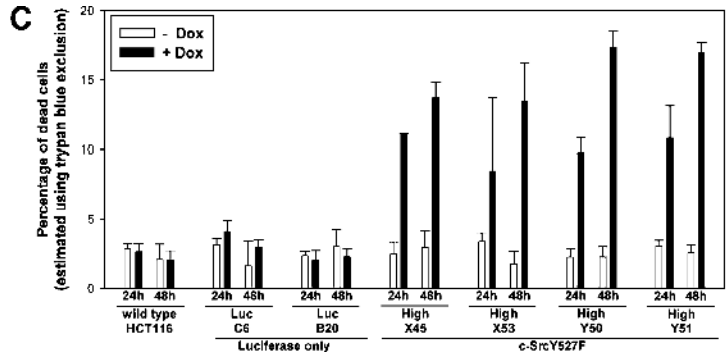
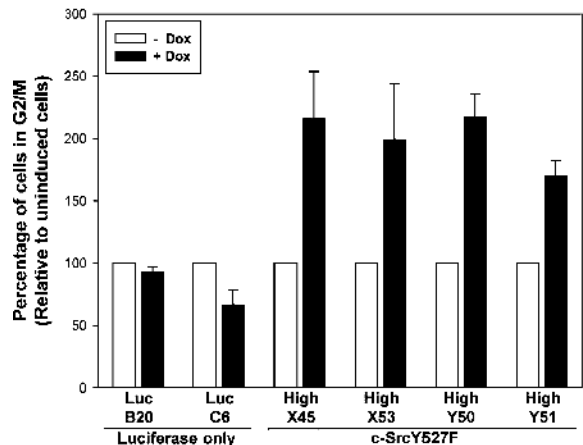
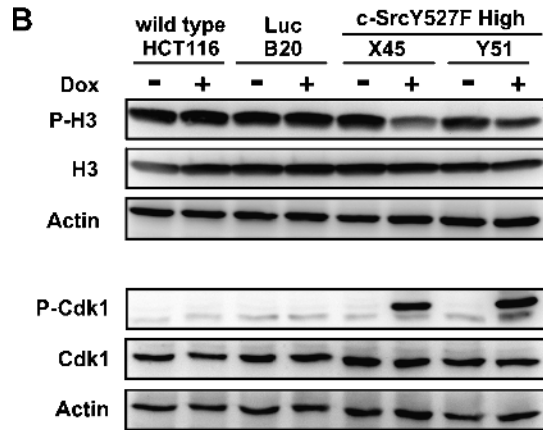
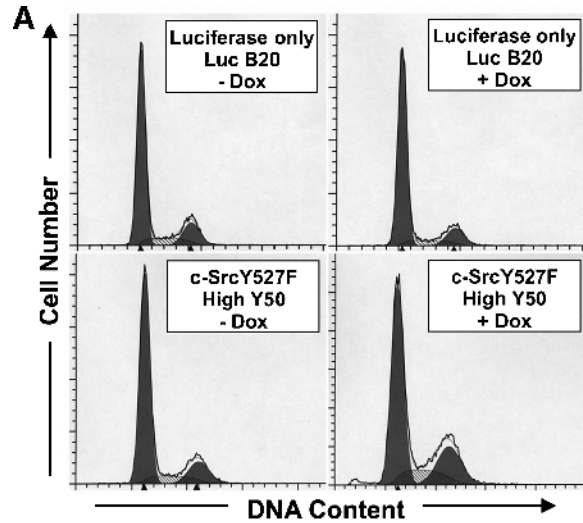
Figure 3. Consequences of the high-level induction of c-SrcY527F in HCT116 colorectal cancer cells. (A) Representative pictures of HCT116 Luc-Src527F High (clone HighY50) and control HCT116 Luc-only (clone LucC6) cells 24 hours after induction. Fluorescent microscopy insert illustrates lack of EGFP signals in vesicles formed after a high-level expression of c-SrcY527F. (B) Western blot analyses showing increases in the expression level of total and autophosphorylated c-Src [Tyr416] 24 hours after induction in HCT116 Luc-Src527F High clones but not in HCT116 Luc-only controls and wt HCT116 cells. (C) Quantification of adherent and detached cells in indicated Dox-induced and uninduced HCT116 Luc-Src527F High clones, HCT116 Luc-only control cell lines, and parental HCT116 wt cells. Cell counts were performed 24 hours after induction, and data are based on three independent experiments performed in triplicate. All HCT116 Luc-Src527F High clones displayed significantly decreased total cell numbers and increased numbers of detached cells following induction with Dox (two-sided t-tests, $P < .01$). A slight decrease in total cell number following Dox treatment was also observed for clone HCT116 Luc-only C6 ($P < .05$), but this was caused by a mechanism different from that observed for HCT116 Luc-Src527F High clones (Figure 4). (D) Four-day growth curves of HCT116 Luc-Src527F HighY50 cells, and HCT116 Luc-only, and LucB20 controls grown in the absence and in the presence of Dox. The initial seeding density was 4×10^5 cells/well. Data are representative of three independent experiments performed in triplicate.

SMVLuc-Src527F HighY50, respectively) as xenografts in nude mice. As illustrated in Figure 7, neither induction of wt c-Src nor induction of c-SrcY527F resulted in any growth-promoting effects in HCT116 tumor xenografts. If anything, tumors induced to express c-SrcY527F displayed growth slower than those of their uninduced counterparts (Figure 7B). Taken together, these data suggest that increases

in c-Src levels and activity are unlikely to promote the growth of HCT116 cells *in vivo*.

Discussion

A large body of evidence links aberrant Src signaling to the development and progression of a variety of human tumors,



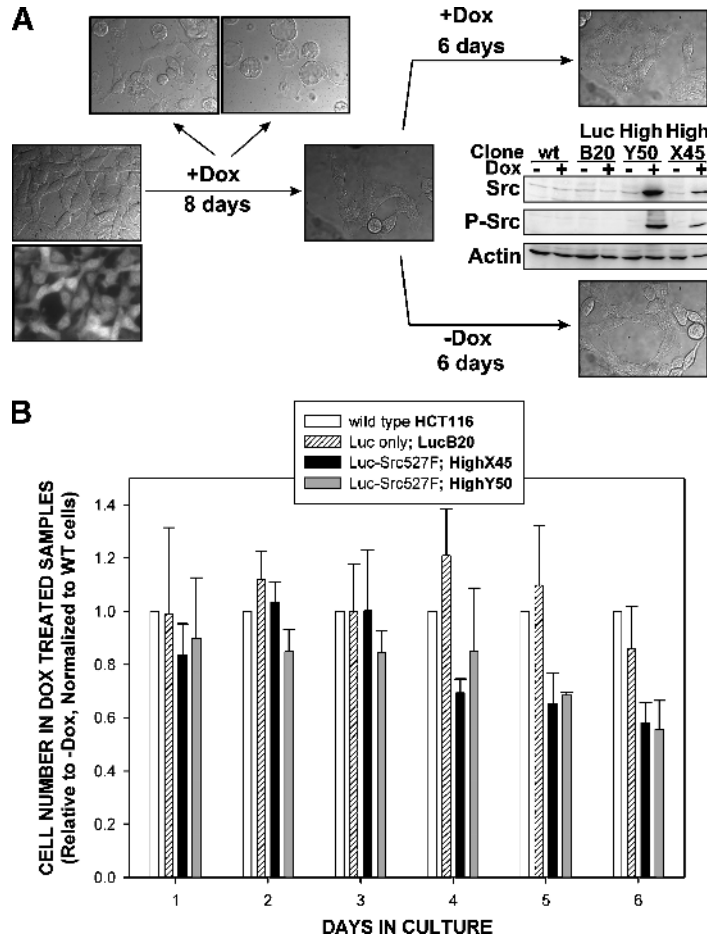


Figure 5. Increased levels and activity of Src do not promote the growth of the fraction of HCT116 Luc-Src527F cells that overcame the growth delay induced by a high-level expression of c-SrcY527F. (A) Schematic illustrating the generation and morphologic properties of "post-growth-delay" cells. Western blot analyses show the levels of total and autophosphorylated [Tyr416] Src in "post-growth-delay" cells and matched controls grown for 6 days in the presence or in the absence of Dox (end point of experiments presented in B). (B) Growth properties of "post-growth-delay" HCT116 Luc-Src527F High cells (clones HighX45 and HighY50) maintained for 6 days in the presence or in the absence of Dox. Identically treated HCT116 Luc-only cells (clone LucB20) and wt HCT116 cells were used as controls. The initial seeding density was 1×10^5 cells/well in a six-well plate, and the medium was replaced by fresh medium on day 3. For each day, data are presented as the ratio of total cell number in the presence of Dox to the total number of the same cells in the absence of Dox, and are normalized to the results obtained with wt HCT116 cells. Normalization was performed to compensate for unspecific inhibitory effects of prolonged Dox treatment. Data are representative of three independent experiments performed in triplicate.

making c-Src an attractive target for cancer chemotherapy [2,5–7,30]. Indeed, small molecule inhibitors of c-Src display anticancer activity *in vitro* and in xenograft models in several experimental systems, and candidate drugs are approaching or have recently entered phase I clinical trials worldwide [31]. The success and efficiency of Src-focused therapeutic strategies rely on a thorough understanding of Src function in

relevant human cancer cell contexts. Until very recently, the majority of function testing studies of Src were performed in fibroblasts and/or used the viral homologue v-Src, rather than the c-Src proto-oncogene [2]. Human cancers are predominantly of epithelial origin and, in recent years, it has become evident that epithelial cells differ from fibroblasts in many aspects of cellular behavior [32,33]. Thus, there is a pressing

Figure 4. Effects of a high-level induction of c-SrcY527F on cell cycle profile and cell viability in HCT116 colorectal carcinoma cells. (A) Cell cycle profiles of HCT116 Luc-only cells (clone LucB20) and HCT116 Luc-Src527F cells (clone HighY50) obtained after 24 hours of growth in the presence or in the absence of Dox. Data are representative of three independent experiments. Results obtained with other Luc-only and Luc-Src527F High clones analyzed were similar to those using clones LucB20 and Luc-Src527F HighY50, respectively. (B) Histogram illustrating relative increases in the percentage of cells in the G₂/M phase of the cell cycle after 24 hours of growth in the presence of Dox in HCT116 Luc-Src527F High cells but not in control HCT116 Luc-only clones. Data are based on three independently obtained cell cycle profiles. Western blot analyses show an accompanying decrease in levels of phosphorylated histone H3 [P-Ser10] and an increase in the phosphorylation of Cdk1 [P-Tyr15], confirming the accumulation of cells in the G₂ phase rather than in the M phase of the cell cycle [38]. They are representative of three repeat experiments. (C) Increases in the percentage of dead cells 24 and 48 hours after induction with Dox in HCT116 Luc-Src527F High cells but not in control clones. Determined using trypan blue exclusion method. Representative of three independent experiments performed in triplicate. (D) Histogram illustrating the levels of apoptosis-associated M30 antigen in the conditioned medium of indicated HCT116 Luc-Src527F High clones, control Luc-only cell lines, and parental wt HCT116 cells grown for 24 hours in the absence or in the presence of Dox. Staurosporine (35 nM)-treated cells represent positive control for ~50% apoptotic cells. Data are representative of three independent experiments performed in triplicate. Lack of apoptotic phenotype following a high-level induction of c-SrcY527F was also independently confirmed by DAPI staining (Figure W3). (E) Representative electron microscopy pictures illustrating ultrastructural changes occurring in HCT116 cells following a high-level induction of c-SrcY527F.

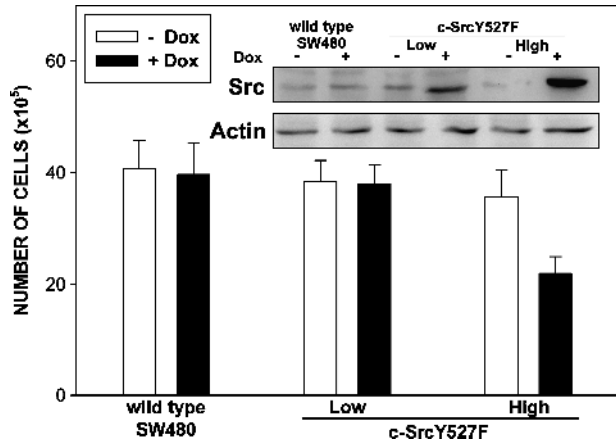


Figure 6. Consequences of low-level and high-level induction of c-SrcY527F in SW480 colorectal cancer cells. Histogram shows cell numbers in induced and uninduced SW480 Luc-Src527F Low, SW480 Luc-Src527F High, and parental SW480 cells 24 hours after Dox treatment. Data are based on three independent experiments performed in triplicate. SW480 Luc-SrcY527F High cells displayed a significantly decreased total cell number following induction with Dox compared to noninduced cells (two-sided t-test, $P < .05$). No statistically significant differences were found between the numbers of wt SW480 and SW480 Luc-Src527F Low cells in the presence and in the absence of Dox ($P > .05$). Western blot analysis illustrates increases in the amount of Src following Dox induction.

Our results clearly demonstrate that elevations in c-Src levels and activity do not promote the proliferation of HCT116 and SW480 cells. In fact, we have shown that a constitutively active mutant of c-Src (c-SrcY527F) might have growth-inhibitory consequences if expressed at very high levels. These data contrast with proliferation-promoting effects of the overexpression of v-Src and c-SrcY527F in fibroblasts and further substantiate the need for more detailed studies on the role of c-Src in cell cycle progression in defined human epithelial cell contexts. Although we cannot exclude that inducing Src might trigger proliferative response in some other colorectal cancer cell types, based on the results presented, it seems reasonable to speculate that there might be no simple correlation between c-Src level/activity and the growth rate of tumor cells in the late stages of colorectal carcinogenesis. Consequently, in advanced colorectal carcinomas, c-Src inhibitors might be more effective than tumor growth in suppressing other processes (e.g., invasion and metastasis). Indeed, there is emerging evidence in support of such scenario [16]. It is still possible, however, that c-Src promotes cell proliferation at earlier phases of colorectal carcinogenesis (e.g., at dysplastic epithelium stage) and that a certain level of endogenous c-Src activity is required for the continued growth of colorectal carcinoma cells. In this respect, there are reports that c-Src might be involved in tumor angiogenesis and that inhibiting c-Src activity can suppress cancer cell growth [34–36]. Without doubt, further studies are required to fully characterize the role of c-Src at diverse stages of colorectal carcinogenesis. Such studies might provide invaluable insights into c-Src function and help to optimize the use of Src inhibitors in colorectal cancer therapy.

need to further assess Src function(s) in experimental models relevant to those human cancers in which Src is over-expressed. We developed a single-step inducible gene expression approach (SMV system) and applied it to investigate the consequences of increasing c-Src levels and activity on the growth of human colorectal cancer cells.

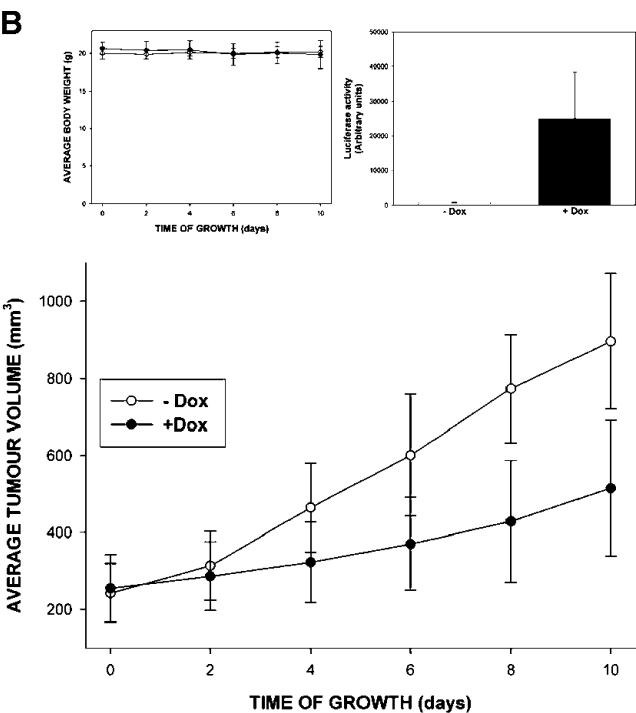
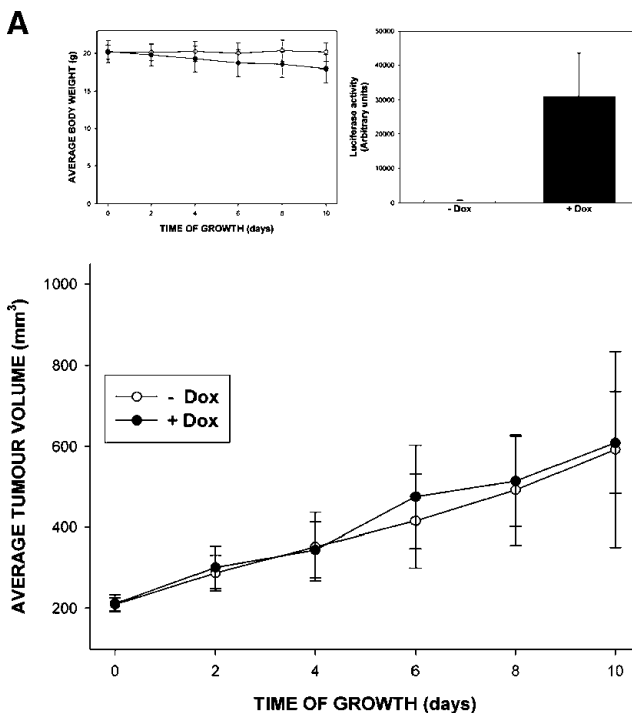


Figure 7. Consequences of the induction of wt c-Src (A) and c-SrcY527F (B) on the growth of HCT116 cells in a xenograft model. There were at least five animals in each control group and Dox-treated group. Successful gene induction in Dox-treated animals was confirmed using luciferase reporter assay (histogram insert). The use of a Dox-containing diet did not affect animal body weight during the experiment (line-plot insert).

Supplementary Information for Materials and Methods

Electron Microscopy Studies

Trypsinized adherent cells and detached cells obtained 48 hours after Dox treatment were spun gently (for 3 minutes at 800 rpm in a standard bench-top centrifuge) and washed twice or thrice with freshly prepared Soerensen's buffer. [This is obtained by adding 95 ml of KH_2PO_4 solution (2.04 g/100 ml) to 405 ml of Na_2HPO_4 ($-2\text{H}_2\text{O}$) solution (13.34 g/500 ml), which results in a 0.15-M buffer at pH 7.4.] The cells were fixed with 2.5% glutaraldehyde and 1% OsO_4 (each fixative was prepared in Soerensen's buffer). Each fixation step took 1 hour and was followed by three washes with Soerensen's buffer. The samples were subsequently dehydrated by incubation (5 minutes each) in increasing concentrations of ethanol (30%, 50%, 70%, 95%, and 100%; $\times 3$). This was followed by embedding in Spurr's resin [1]. Infiltration steps were performed as follows: 1:3 resin/acetone for 1 hour; 1:1 resin/acetone for 1 hour; 3:1 resin/acetone for 1 hour; 100% resin for 1 hour; 100% resin overnight. Samples were subsequently embedded in fresh resin in Beem capsules 00 (Agar Scientific Ltd., Stansed, UK) for 48 hours at 70°C. Sections were cut at a thickness of 60 nm using an Ultratrim 45 diamond knife (Diatome, Biel, Switzerland) mounted on a Leica Ultracut S (Leica Microsystems AG, Wetzlar, Austria) and collected on 200-mesh 3.05-mm copper grids (Agar Scientific Ltd.). Sections were poststained, 5 minutes in each, with 2% uranyl acetate in 70% ethanol followed by Reynolds lead citrate [2]. Sections were imaged on a JEOL 1220 TEM (JEOL UK Ltd., Welwyn Garden City, UK) at an accelerating voltage of 80 kV, and images were collected using a SiS Megaview II CCD camera (Soft Imaging Systems GmbH, Munster, Germany).

Cell Cycle Analysis

For cell cycle analysis, 7.89×10^5 cells were seeded into duplicate T75 tissue culture flasks. Three days later, when cells were in the logarithmic phase of growth as determined by growth curves (Figure W4), Dox was added to one of the flasks, and both were harvested 24 hours later. They were then trypsinized, counted, and adjusted to a density of 2×10^6 cells/ml (final volume). Cells were spun at 350g for 4 minutes, the medium was aspirated, and 1.3 ml of ice-cold PBS was added while vortexing. Three milliliters of absolute ethanol (at -20°C) was added while vortexing (i.e., final mixture, 70% ethanol). Cells were left for fixing overnight at 4°C. Cells were resuspended in 1 ml of PBS containing 20 $\mu\text{g/ml}$ propidium iodide (cat. no. P4864; Sigma) and 1 $\mu\text{g/ml}$ RNase A (cat. no. R4875; Sigma), and incubated at 37°C for 30 minutes. Flow cytometry was performed on a Becton Dickinson FACSCalibur machine (Becton Dickinson, San Jose, CA) set at 4250-mV excitation using a 488-nm laser line. Forward scatter and orthogonal light scatter were collected together with red fluorescence (DNA-bound propidium iodide; 585 ± 21 nm, linear scale). Cell clumps were excluded by fluorescence pulse processing. Cell cycle analysis of collected data was performed using ModFitLT Version 2.0 software (Verity Software House, Topsham, ME).

Acknowledgements

We would like to thank Jeff Barry and Mike Hughes for their technical assistance with flow cytometry, and Deema Hussein for help with cell cycle analysis. Cassandra Hodgkinson is acknowledged for her help with xenograft experiments.

References

- [1] Martin GS (2001). The hunting of the Src. *Nat Rev Mol Cell Biol* **2**, 467–475.
- [2] Yeatman TJ (2004). A renaissance for SRC. *Nat Rev Cancer* **4**, 470–480.
- [3] Thomas SM and Brugge JS (1997). Cellular functions regulated by Src family kinases. *Annu Rev Cell Dev Biol* **13**, 513–609.
- [4] Erpel Tand Courtneidge SA (1995). Src family protein tyrosine kinases and cellular signal transduction pathways. *Curr Opin Cell Biol* **7**, 176–182.
- [5] Frame MC (2002). Src in cancer: deregulation and consequences for cell behaviour. *Biochim Biophys Acta* **1602**, 114–130.
- [6] Summy JM and Gallick GE (2003). Src family kinases in tumor progression and metastasis. *Cancer Metastasis Rev* **22**, 337–358.
- [7] Russello SV and Shore SK (2004). SRC in human carcinogenesis. *Front Biosci* **9**, 139–144.
- [8] Talamonti MS, Roh MS, Curley SA, and Gallick GE (1993). Increase in activity and level of pp60c-src in progressive stages of human colorectal cancer. *J Clin Invest* **91**, 53–60.
- [9] Cartwright CA, Meisler AI, and Eckhart W (1990). Activation of the pp60c-src protein kinase is an early event in colonic carcinogenesis. *Proc Natl Acad Sci USA* **87**, 558–562.
- [10] Bolen JB, Veillette A, Schwartz AM, Deseau V, and Rosen N (1987). Analysis of pp60c-src in human colon carcinoma and normal human colon mucosal cells. *Oncogene Res* **1**, 149–168.
- [11] Mao W, Irby R, Coppola D, Fu L, Wloch M, Turner J, Yu H, Garcia R, Jove R, and Yeatman TJ (1997). Activation of c-Src by receptor tyrosine kinases in human colon cancer cells with high metastatic potential. *Oncogene* **15**, 3083–3090.
- [12] Aligayer H, Boyd DD, Heiss MM, Abdalla EK, Curley SA, and Gallick GE (2002). Activation of Src kinase in primary colorectal carcinoma: an indicator of poor clinical prognosis. *Cancer* **94**, 344–351.
- [13] Avizienyte E, Wyke AW, Jones RJ, McLean GW, Westhoff MA, Brunton VG, and Frame MC (2002). Src-induced de-regulation of E cadherin in colon cancer cells requires integrin signalling. *Nat Cell Biol* **4**, 632–638.
- [14] Irby RB and Yeatman TJ (2002). Increased Src activity disrupts cadherin/catenin-mediated homotypic adhesion in human colon cancer and transformed rodent cells. *Cancer Res* **62**, 2669–2674.
- [15] Jones RJ, Avizienyte E, Wyke AW, Owens DW, Brunton VG, and Frame MC (2002). Elevated c-Src is linked to altered cell-matrix adhesion rather than proliferation in KM12C human colorectal cancer cells. *Br J Cancer* **87**, 1128–1135.
- [16] Nam JS, Ino Y, Sakamoto M, and Hirohashi S (2002). Src family kinase inhibitor PP2 restores the E-cadherin/catenin cell adhesion system in human cancer cells and reduces cancer metastasis. *Clin Cancer Res* **8**, 2430–2436.
- [17] Sakamoto M, Takamura M, Ino Y, Miura A, Genda T, and Hirohashi S (2001). Involvement of c-Src in carcinoma cell motility and metastasis. *Jpn J Cancer Res* **92**, 941–946.
- [18] Cartwright CA, Eckhart W, Simon S, and Kaplan PL (1987). Cell transformation by pp60c-src mutated in the carboxy-terminal regulatory domain. *Cell* **49**, 83–91.
- [19] Kmiecik TE and Shalloway D (1987). Activation and suppression of pp60c-src transforming ability by mutation of its primary sites of tyrosine phosphorylation. *Cell* **49**, 65–73.
- [20] Riley D, Carragher NO, Frame MC, and Wyke JA (2001). The mechanism of cell cycle regulation by v-Src. *Oncogene* **20**, 5941–5950.
- [21] Irby R, Mao W, Coppola D, Jove R, Gamero A, Cuthbertson D, Fujita DJ, and Yeatman TJ (1997). Overexpression of normal c-Src in poorly metastatic human colon cancer cells enhances primary tumor growth but not metastatic potential. *Cell Growth Differ* **8**, 1287–1295.
- [22] Gayet J, Zhou XP, Duval A, Rolland S, Hoang JM, Coutu P, and Hamelin R (2001). Extensive characterization of genetic alterations in a series of human colorectal cancer cell lines. *Oncogene* **20**, 5025–5032.
- [23] Welman A, Cawthorne C, Barraclough J, Smith N, Griffiths GJ, Cowen RL, Williams JC, Stratford IJ, and Dive C (2005). Construction and characterization of multiple human colon cancer cell lines for inducibly regulated gene expression. *J Cell Biochem* **94**, 1148–1162.

- [24] Welman A, Burger MM, and Hagmann J (2000). Structure and function of the C-terminal hypervariable region of K-Ras4B in plasma membrane targeting and transformation. *Oncogene* **19**, 4582–4591.
- [25] Reipert S, Bennion G, Hickman JA, and Allen TD (1999). Nucleolar segregation during apoptosis of haemopoietic stem cell line FDCP-Mix. *Cell Death Differ* **6**, 334–341.
- [26] Kramer G, Erdal H, Mertens HJ, Nap M, Mauermann J, Steiner G, Marberger M, Biven K, Shoshan MC, and Linder S (2004). Differentiation between cell death modes using measurements of different soluble forms of extracellular cytokeratin 18. *Cancer Res* **64**, 1751–1756.
- [27] Welman A, Barraclough J, and Dive C (2006). Generation of cells expressing improved doxycycline regulated reverse transcriptional transactivator rTA2S-M2. *Nat Protoc* **1**, 803–811.
- [28] Dehm S, Senger MA, and Bonham K (2001). SRC transcriptional activation in a subset of human colon cancer cell lines. *FEBS Lett* **487**, 367–371.
- [29] Allgayer H, Wang H, Gallick GE, Crabtree A, Mazar A, Jones T, Kraker AJ, and Boyd DD (1999). Transcriptional induction of the urokinase receptor gene by a constitutively active Src. Requirement of an upstream motif (–152/–135) bound with Sp1. *J Biol Chem* **274**, 18428–18437.
- [30] Irby RB and Yeatman TJ (2000). Role of Src expression and activation in human cancer. *Oncogene* **19**, 5636–5642.
- [31] Summy JM and Gallick GE (2006). Treatment for advanced tumors: SRC reclaims center stage. *Clin Cancer Res* **12**, 1398–1401.
- [32] Skinner J, Bounacer A, Bond JA, Haughton MF, deMicco C, and Wynford-Thomas D (2004). Opposing effects of mutant ras oncoprotein on human fibroblast and epithelial cell proliferation: implications for models of human tumorigenesis. *Oncogene* **23**, 5994–5999.
- [33] Rangarajan A, Hong SJ, Gifford A, and Weinberg RA (2004). Species- and cell type-specific requirements for cellular transformation. *Cancer Cell* **6**, 171–183.
- [34] Moasser MM, Srethapakdi M, Sachar KS, Kraker AJ, and Rosen N (1999). Inhibition of Src kinases by a selective tyrosine kinase inhibitor causes mitotic arrest. *Cancer Res* **59**, 6145–6152.
- [35] Staley CA, Parikh NU, and Gallick GE (1997). Decreased tumorigenicity of a human colon adenocarcinoma cell line by an antisense expression vector specific for c-Src. *Cell Growth Differ* **8**, 269–274.
- [36] Park J and Cartwright CA (1995). Src activity increases and Yes activity decreases during mitosis of human colon carcinoma cells. *Mol Cell Biol* **15**, 2374–2382.
- [37] Parhamifar L, Jeppsson B, and Sjolander A (2005). Activation of cPLA2 is required for leukotriene D4-induced proliferation in colon cancer cells. *Carcinogenesis* **26**, 1988–1998.
- [38] Smits VA and Medema RH (2001). Checking out the G(2)/M transition. *Biochim Biophys Acta* **1519**, 1–12.

Supplementary Information

- [1] Spur AR (1969). A low viscosity epoxy resin embedding medium for electron microscopy. *J Ultrastruct Res* **26**, 31–43.
- [2] Reynolds ES (1963). The use of lead citrate at high pH as an electron-opaque stain in electron microscopy. *J Cell Biol* **17**, 208–212.

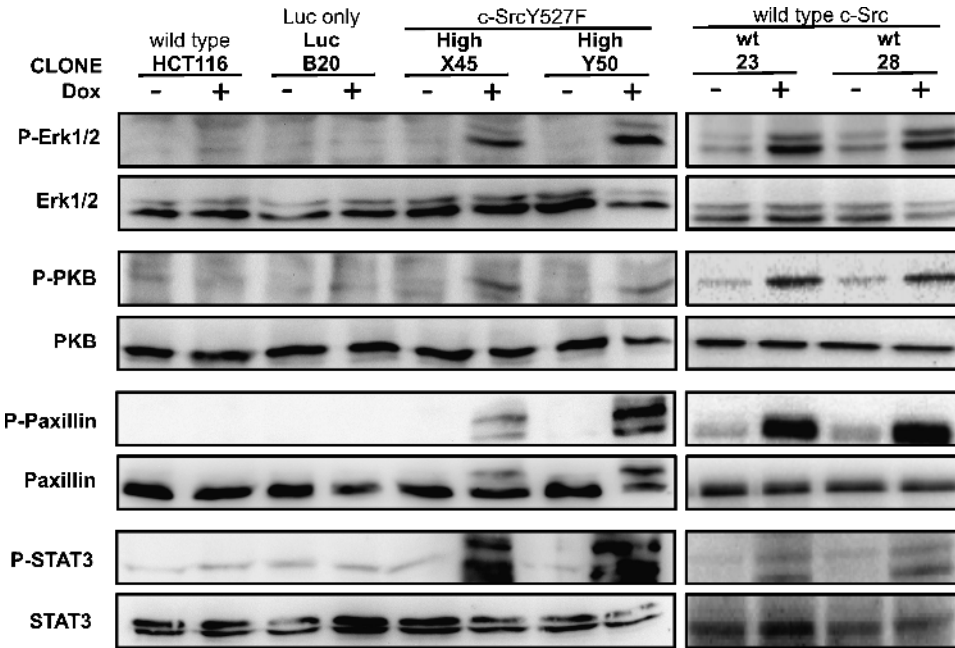


Figure W1. Western blot analyses illustrating the phosphorylation of selected downstream effectors of c-Src in indicated HCT116 clones grown for 24 hours in the presence or in the absence of induction. Results are representative of at least two independent cell preparations.

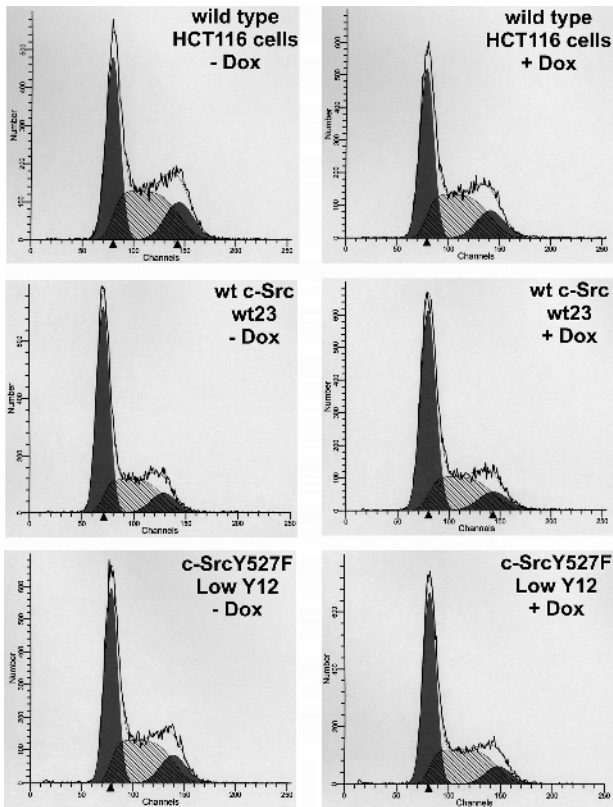


Figure W2. Cell cycle profiles of parental HCT116 cells, HCT116 LucwtSrc cells (clone wt23), and HCT116 Luc-Src527F Low cells (clone LowY12) obtained after 24 hours of growth in the presence or in the absence of Dox. Data are representative of three independent experiments.

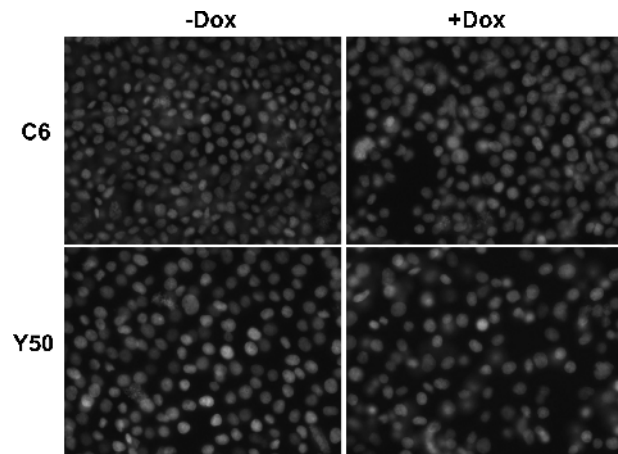


Figure W3. Representative pictures showing lack of apoptotic nuclei among HCT116 Luc-Src527F cells (clone High Y50) and HCT116 Luc-only control cells (clone Luc C6) irrespective of Dox induction. Similar results have been obtained with other clones tested.

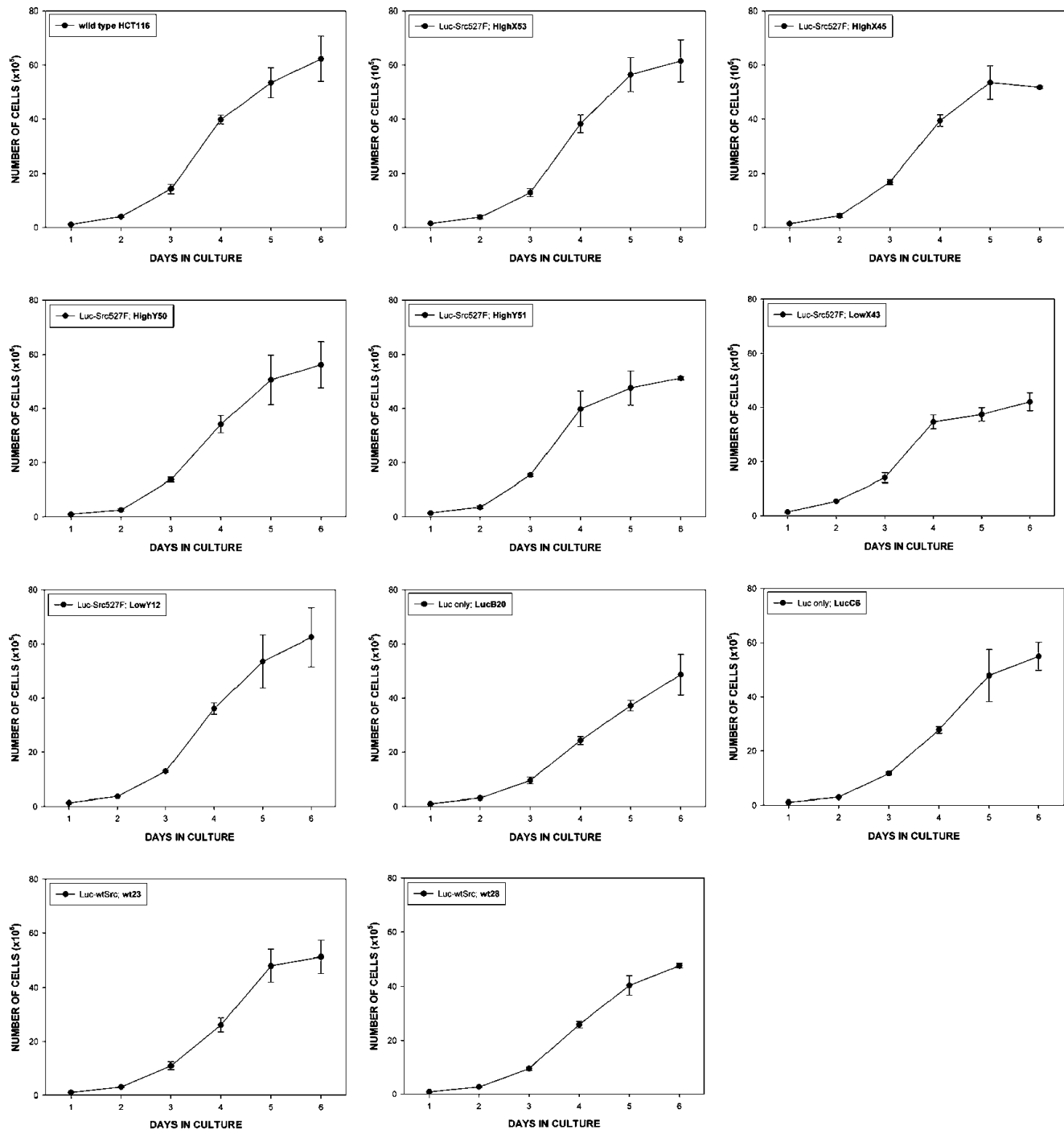


Figure W4. Growth curves from Figure 1D presented individually for each clone.